

# Optimization of reaction conditions for cyclohexene epoxidation with $\text{H}_2\text{O}_2$ over nanocrystalline mesoporous $\text{TiO}_2$ loaded with $\text{RuO}_2$

Thammanoon Sreethawong<sup>a,1</sup>, Yusuke Yamada<sup>b,\*</sup>,  
Tetsuhiko Kobayashi<sup>b</sup>, Susumu Yoshikawa<sup>a,\*\*</sup>

<sup>a</sup> Institute of Advanced Energy, Kyoto University, Uji, Kyoto 611-0011, Japan

<sup>b</sup> Research Institute for Ubiquitous Energy Devices, National Institute of Advanced Industrial Science and Technology (AIST),  
1-8-31 Midorigaoka, Ikeda, Osaka 563-8577, Japan

Received 27 July 2005; received in revised form 21 December 2005; accepted 22 December 2005

Available online 7 February 2006

## Abstract

Cyclohexene epoxidation with  $\text{H}_2\text{O}_2$  was performed over  $\text{RuO}_2/\text{TiO}_2$  under various conditions. The support  $\text{TiO}_2$  prepared by surfactant-assisted templating sol–gel method is nanocrystalline and has mesoporous structure with narrow monomodal pore size distribution. An activator of 1 mol%  $\text{RuO}_2$  was loaded onto the synthesized  $\text{TiO}_2$  by incipient wetness impregnation method. The resultant catalyst was characterized by XRD,  $\text{N}_2$  adsorption–desorption and TEM analyses. Reaction conditions in the epoxidation reaction, namely reaction temperature, amount of catalyst and concentration of  $\text{H}_2\text{O}_2$  in terms of cyclohexene/ $\text{H}_2\text{O}_2$  ratio, were systematically optimized to obtain maximum selectivity to cyclohexene oxide. © 2006 Elsevier B.V. All rights reserved.

**Keywords:** Mesoporosity;  $\text{RuO}_2/\text{TiO}_2$ ; Epoxidation; Cyclohexene;  $\text{H}_2\text{O}_2$

## 1. Introduction

Nanocrystalline mesoporous  $\text{TiO}_2$  generally possesses high catalytic efficiency because of its unique properties conferred by very small physical dimensions [1–3]. The large specific surface area and high volume fraction of atoms located both on the surface and at the grain boundaries result in an increased surface energy. Then, the surface of nanocrystalline  $\text{TiO}_2$  provides an active substrate for catalysis [4]. In addition, the reactants are operated across the porous system in several applications, sufficiently uniform pore size of 2–50 nm in the mesopore region is more suitable if loading of cocatalysts/dopants is required as not to become easily blocked as in the case of microporous materials (pore size < 2 nm) [5]. Therefore, the surface

of nanocrystalline  $\text{TiO}_2$  particles with a mesoporous structural network will be more promising because catalytic activity can be further enhanced due to the enlarged surface area for facilitating better reactant accessibility to the catalysts and subsequent surface reactions [6].

Epoxidation reactions are indispensable for the chemical industry in order to produce important chemical intermediates. Unlike ordinary ethers, epoxides are quite reactive. The strained three-membered ring easily reacts with a nucleophile. By the reaction with a wide variety of nucleophiles, epoxides can be transformed into useful chemicals [7,8]. Production of epoxide by the reaction of alkenes with hydrogen peroxide ( $\text{H}_2\text{O}_2$ ) is an ideal synthetic route since  $\text{H}_2\text{O}_2$  is easy for handling and inexpensive, and possesses high content of active oxygen [9].

Alkene epoxidation with  $\text{H}_2\text{O}_2$  generally requires a catalyst. In particular, a class of cyclohexene oxide is an important organic intermediate consumed in the production of pharmaceuticals, plant-protection agents, pesticides and stabilizers for chlorinated hydrocarbons [10]. Much effort has been dedicated to the development of new active and selective catalysts for cyclohexene epoxidation that circumvent the formation of large amounts of by-products because several side reactions can take place, such as oxidation in the allylic positions, ring-opening of the epoxides

\* Corresponding author. Tel.: +81 72 751 9656; fax: +81 72 751 9630.

\*\* Corresponding author. Tel.: +81 774 38 3504; fax: +81 774 38 3508.

E-mail addresses: [thammanoon.s@chula.ac.th](mailto:thammanoon.s@chula.ac.th) (T. Sreethawong),  
[Yusuke.YAMADA@aist.go.jp](mailto:Yusuke.YAMADA@aist.go.jp) (Y. Yamada), [s-yoshi@iae.kyoto-u.ac.jp](mailto:s-yoshi@iae.kyoto-u.ac.jp)  
(S. Yoshikawa).

<sup>1</sup> Present address: The Petroleum and Petrochemical College, Chulalongkorn University, Soi Chula 12, Phythai Road, Pathumwan, Bangkok 10330, Thailand. Tel.: +66 2 218 4132; fax: +66 2 215 4459.

by hydrolysis or solvolysis, epoxide rearrangement or even total breakdown of the C=C double bonds. Cyclohexene epoxidation to yield cyclohexene oxide is also one of the most difficult cases since the first two problems, namely allylic oxidation and epoxide ring-opening, occur considerably [11].

So far, the utilization of RuO<sub>2</sub> in catalysis field has been considerably focused for a plenty of reactions by being loaded on various kinds of support, such as RuO<sub>2</sub>/TiO<sub>2</sub> [12], RuO<sub>2</sub>/Fe<sub>2</sub>O<sub>3</sub> [13], RuO<sub>2</sub>/WO<sub>3</sub> [14], RuO<sub>2</sub>/M<sub>2</sub>Sb<sub>2</sub>O<sub>7</sub> (M = Ca, Sr) [15] and RuO<sub>2</sub>/zeolite Y [16] for water splitting reaction, RuO<sub>2</sub>/Al<sub>2</sub>O<sub>3</sub> for wet air oxidation of ammonia [17] and RuO<sub>2</sub>/CeO<sub>2</sub> for wet oxidation of acetic acid [18]. To our knowledge, it (in oxide form of RuO<sub>2</sub>) has not yet been applied for any epoxidation reactions. However, only Ru in many complex forms has been extensively used for numerous epoxidation reactions, such as epoxidation of propene, octene, cyclohexene, cyclooctene, styrene, etc. [19–26]. Therefore, it is a good probability to extend the application of supported RuO<sub>2</sub> for the first time in catalytic cyclohexene epoxidation.

In our previous works, nanocrystalline mesoporous TiO<sub>2</sub> prepared by a surfactant-assisted templating sol–gel process [27] was used for cyclohexene epoxidation for the first time. The mesoporous TiO<sub>2</sub> showed superior catalytic performance for cyclohexene epoxidation to non-mesoporous commercial TiO<sub>2</sub> powders. Its catalytic performance was drastically enhanced by loading with RuO<sub>2</sub> at optimum content of 1 mol%, resulting in high selectivity to cyclohexene oxide [28]. In this contribution, the RuO<sub>2</sub>-loaded nanocrystalline mesoporous TiO<sub>2</sub> catalyst was utilized to examine the effects of several reaction parameters in the cyclohexene epoxidation reaction in order to attain optimized conditions for maximum cyclohexene oxide selectivity.

## 2. Experimental

### 2.1. Catalyst preparation

Synthesis procedure of nanocrystalline mesoporous TiO<sub>2</sub> has been reported previously [27,28]. RuO<sub>2</sub>-loaded TiO<sub>2</sub> catalyst was prepared by an incipient wetness method with an appropriate amount of aqueous solution of Ru(NO)(NO<sub>3</sub>)<sub>3</sub>. The impregnated TiO<sub>2</sub> catalyst was then dried at 80 °C and finally calcined at 500 °C for 6 h.

### 2.2. Catalyst characterizations

X-ray diffraction (XRD) was used to identify phases present in the samples. A Rigaku RINT-2100 rotating anode XRD system generating monochromated Cu K $\alpha$  radiation with continuous scanning mode at rate of 2° min<sup>-1</sup> and operating conditions of 40 kV and 40 mA was used to obtain XRD pattern. A nitrogen adsorption system (BEL Japan BELSORP-18 Plus) was employed to measure adsorption–desorption isotherms at liquid nitrogen temperature of –196 °C. The Brunauer–Emmett–Teller (BET) approach using adsorption data over the relative pressure ranging from 0.05 to 0.35 was utilized to determine specific surface area. The Barrett–Joyner–Halenda (BJH) approach was used to yield mean pore size and pore size distribution from

desorption data. The sample was degassed at 200 °C for 2 h to remove physisorbed gases prior to the measurement. The sample morphology was observed by a transmission electron microscope (TEM, JEOL JEM-200CX) operated at 200 kV.

### 2.3. Catalytic activity measurement

The catalytic activity test was carried out without precautions against molecular oxygen in air. Within a round-bottom glass tube placed in a temperature-controlled chamber, the catalyst (10–50 mg) was added to a solution of cyclohexene (0.5 ml, 5 mmol) in *tert*-butanol (5 ml). The reaction mixture was stirred with magnetic stirrer at 1000 rpm and heated until the reaction temperature was finally maintained at a desired value (40–70 °C). The reaction was then started by the addition of an aqueous solution of 30 wt.% H<sub>2</sub>O<sub>2</sub> (0.04–0.79 ml, 0.5–10 mmol) into the mixture. After 3 h of further stirring, aliquot was withdrawn from the reaction mixture, filtered and injected to a gas chromatograph (Shimadzu, GC-14B, PEG-20 M, N<sub>2</sub> as carrier gas) equipped with a flame ionization detector (FID) for determination of products composition. Control experiments, reacting cyclohexene in *tert*-butanol with H<sub>2</sub>O<sub>2</sub> in the absence of catalyst, were also comparatively investigated. Identification of the products was performed using a gas chromatograph–mass spectrometer (Hewlett Packard, G1800A) with an electron ionization detector. The analysis revealed that the main products from the reaction are cyclohexene oxide (desired product), cyclohex-2-en-1-ol (undesired product) and cyclohex-2-en-1-one (undesired product). Selectivity is always calculated with respect to the converted cyclohexene.

## 3. Results and discussion

### 3.1. Catalyst characterizations

The crystalline phases of the synthesized catalyst were investigated using XRD analysis. XRD pattern of the RuO<sub>2</sub>/TiO<sub>2</sub> catalyst is shown in Fig. 1. The main peaks at 2 $\theta$  of 25.2°,

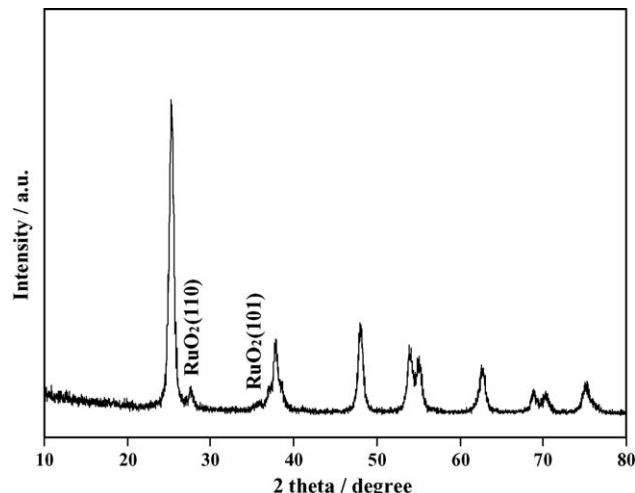


Fig. 1. XRD pattern of RuO<sub>2</sub>/TiO<sub>2</sub> catalyst.

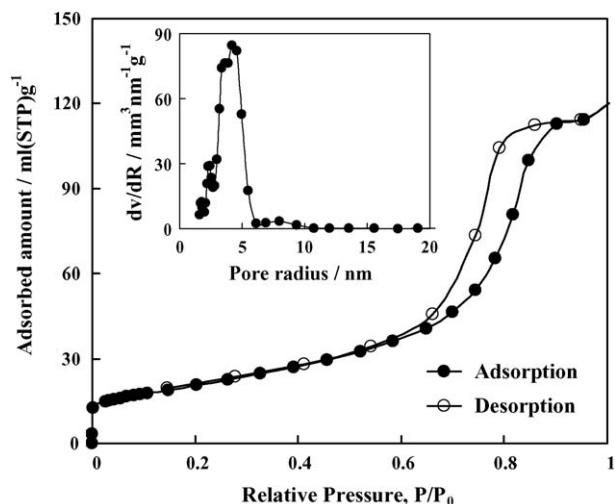


Fig. 2. N<sub>2</sub> adsorption–desorption isotherm and pore size distribution (inset) of RuO<sub>2</sub>/TiO<sub>2</sub> catalyst.

37.9°, 47.8°, 53.8° and 55.0°, which represent the indices of (1 0 1), (0 0 4), (2 0 0), (1 0 5) and (2 1 1) planes, respectively, are ascribed to structure of anatase TiO<sub>2</sub>. The presence of small diffraction peaks at 27.6° and 35.2° is indexed to RuO<sub>2</sub> (1 1 0) and (1 0 1) planes, respectively.

The N<sub>2</sub> adsorption–desorption measurement at liquid N<sub>2</sub> temperature was used to study mesoporosity and textural properties of the RuO<sub>2</sub>/TiO<sub>2</sub> catalyst. Fig. 2 depicts the N<sub>2</sub> adsorption–desorption isotherm and pore size distribution of the RuO<sub>2</sub>/TiO<sub>2</sub>. The isotherm revealed a typical type IV sorption behavior, representing the mesoporous structure characteristic according to the classification of IUPAC [5]. A sharp increase in adsorption volume of N<sub>2</sub> was observed and located in the P/P<sub>0</sub> range of 0.5–0.9. This sharp increase can be attributed to the capillary condensation, indicating the good homogeneity of the sample and fairly small pore size since the P/P<sub>0</sub> position of the inflection point is related to the pore size. As shown in the inset of Fig. 2, the pore size distribution obtained from BJH method showed very narrow and monomodal in the mesopore region (2–50 nm), indicating the good quality of the catalyst prepared by this synthetic system. From N<sub>2</sub> adsorption–desorption and XRD analyses, the synthesized catalyst can be reliably considered as nanocrystalline mesoporous material. The textural properties of the RuO<sub>2</sub>/TiO<sub>2</sub> catalyst are also given in Table 1. The catalyst possessed BET surface area of 73 m<sup>2</sup> g<sup>-1</sup> with mean pore diameter and total pore volume of 8.38 nm and 0.20 cm<sup>3</sup> g<sup>-1</sup>, respectively. When comparing these properties with those of unloaded TiO<sub>2</sub> [28], it can be apparently seen that both the BET surface area and total pore volume decreased with

Table 1  
Textural properties of RuO<sub>2</sub>/TiO<sub>2</sub> catalyst from N<sub>2</sub> adsorption–desorption measurement

Properties	Value
BET surface area (m <sup>2</sup> g <sup>-1</sup> )	73
Mean pore diameter (nm)	8.38
Total pore volume (cm <sup>3</sup> g <sup>-1</sup> )	0.20

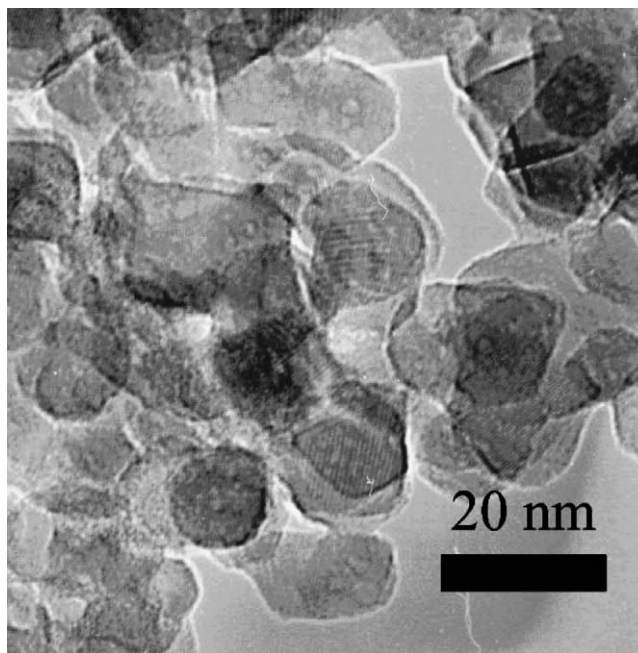
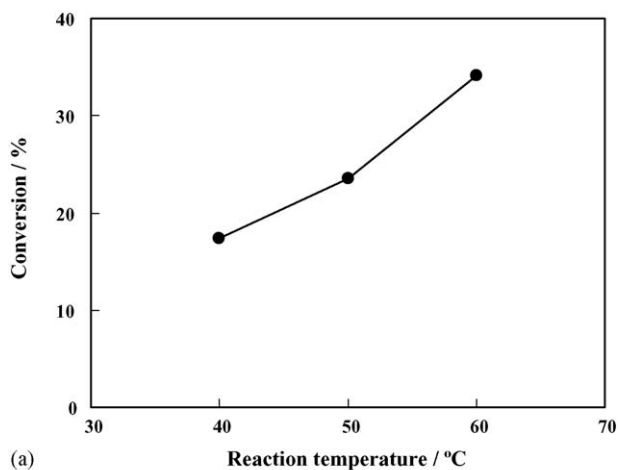


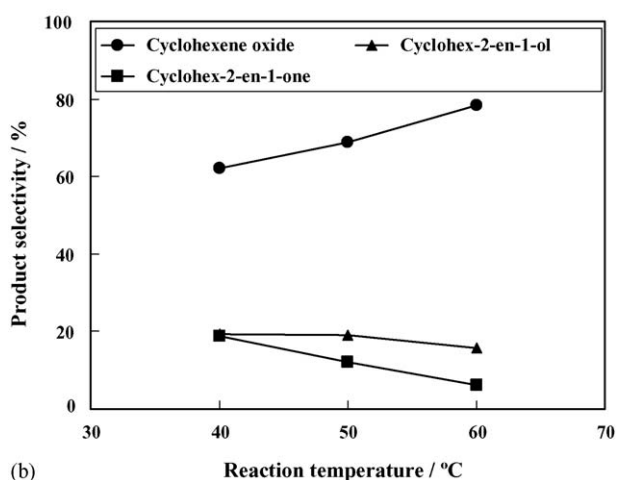
Fig. 3. TEM image of RuO<sub>2</sub>/TiO<sub>2</sub> catalyst.

the RuO<sub>2</sub> loading, but the mean pore size conversely increased as expected. The alteration of these textural properties of the RuO<sub>2</sub>-loaded catalyst can be plausibly owing to the effects of either the blockage of mesopore dimension with deposited RuO<sub>2</sub> particles or the two-step calcination process, which was required for the stabilization of the mesoporous TiO<sub>2</sub> catalyst regarding to the removal of surfactant template prior to the impregnation process and the activation of the RuO<sub>2</sub> additive at the final stage. It can be considered that the former effect might result in the decrement in all properties, whereas the latter effect might cause the decrement in the surface area and total pore volume but the increment in the mean pore size. From the experimental results, the decreased surface area and total pore volume might be attributable to the combination of both of them. However, the increase in mean pore size due to the latter effect might exceed the decrease in mean pore size due to the former effect. Thus, the increased mean pore diameter was eventually observed.

The information about morphological structure of the synthesized catalyst was obtained by TEM analysis. TEM image of the RuO<sub>2</sub>/TiO<sub>2</sub> catalyst shown in Fig. 3 demonstrated the formation of nanocrystalline TiO<sub>2</sub> aggregates composed of three-dimensional disordered primary particles. RuO<sub>2</sub> was observed as deposited particles dispersed on TiO<sub>2</sub> particles. The observed TiO<sub>2</sub> particle sizes of 10–15 nm were consistent with the crystallite size estimated from XRD analysis, elucidating that each grain corresponds in average to a single crystallite. In the same manner, the particle size of the RuO<sub>2</sub> single crystallite was approximately 2–3 nm with some aggregations. Owing to N<sub>2</sub> adsorption–desorption and TEM results, the mesoporous structure of the synthesized catalyst can be attributed to the pores formed between nanocrystalline TiO<sub>2</sub> particles due to their aggregation, which is in the same line as the nanocrystalline mesoporous TiO<sub>2</sub> reported in several literatures [29–33].



(a)



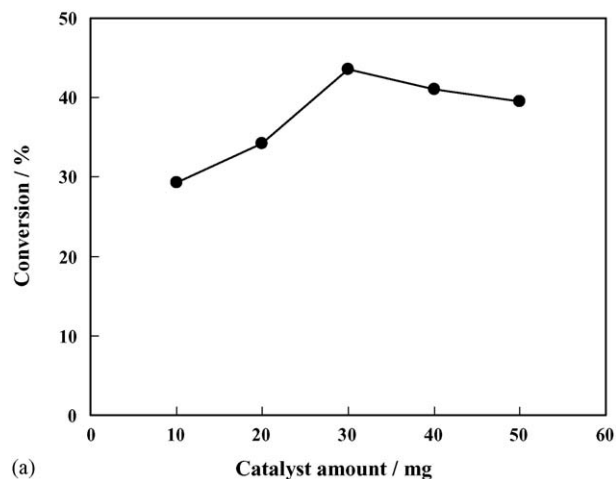
(b)

Fig. 4. Effect of reaction temperature on cyclohexene epoxidation catalyzed by  $\text{RuO}_2/\text{TiO}_2$  catalyst: (a) cyclohexene conversion and (b) product selectivity. Reaction conditions: cyclohexene, 5 mmol;  $\text{H}_2\text{O}_2$ , 1.25 mmol; *tert*-butanol, 5 ml; catalyst, 20 mg; reaction time, 3 h.

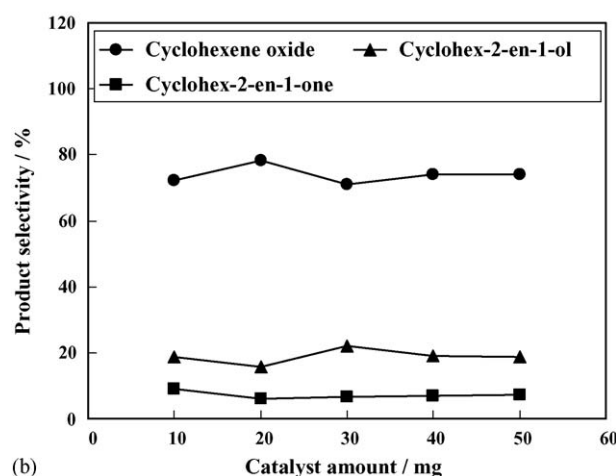
### 3.2. Catalytic activity

From our previous work, the nanocrystalline mesoporous  $\text{TiO}_2$  synthesized by this synthetic method exhibited high potential to be used as cyclohexene epoxidation catalyst, compared with non-mesoporous commercial  $\text{TiO}_2$  powders, i.e. Ishihara ST-01 and Degussa P-25. In addition, the loading of 1 mol% (optimum content) of  $\text{RuO}_2$  onto the mesoporous  $\text{TiO}_2$  significantly enhanced the selectivity to cyclohexene oxide (desired product) [28] when compared to the loading of  $\text{MO}_x$  ( $M = \text{Fe}, \text{Co}, \text{Ni}, \text{V}, \text{Mo}$  and  $\text{W}$ ). Since high selectivity to cyclohexene oxide is focused as a target for developing catalyst, the  $\text{RuO}_2/\text{TiO}_2$  has been taken to improve cyclohexene oxide production by further optimization of reaction conditions.

The effect of reaction temperature was initially studied in the range of 40–60 °C. Over 70 °C, decomposition or vaporization of hydrogen peroxide proceeds suddenly. The results of the effect of the reaction temperature are shown in Fig. 4. It is obviously seen that both conversion and selectivity to cyclohexene oxide drastically decreased with decreasing the reaction temperature from 60 to 40 °C. On the other hand, the selectivities to the



(a)



(b)

Fig. 5. Effect of catalyst amount on cyclohexene epoxidation catalyzed by  $\text{RuO}_2/\text{TiO}_2$  catalyst: (a) cyclohexene conversion and (b) product selectivity. Reaction conditions: cyclohexene, 5 mmol;  $\text{H}_2\text{O}_2$ , 1.25 mmol; *tert*-butanol, 5 ml; reaction temperature, 60 °C; reaction time, 3 h.

other two undesired products (cyclohex-2-en-1-ol and cyclohex-2-en-1-one) increased. This can be inferred that the reaction temperature of 60 °C is an optimum point to yield the highest cyclohexene oxide selectivity under the controllable reaction temperature interval.

The amount of catalyst was further optimized by maintaining the reaction temperature at 60 °C. The catalyst amount was increased up to 50 mg under the identical reaction conditions. The effect of catalyst amount is shown in Fig. 5. The cyclohexene conversion increased with increasing the catalyst amount until reaching the peak at 30 mg and then gradually declined. However, by considering the selectivity to cyclohexene oxide, the catalyst amount of 20 mg provided the highest cyclohexene oxide selectivity of approximately 80%, with minimum selectivities to cyclohex-2-en-1-ol and cyclohex-2-en-1-one. Similar observation has also been reported in case of  $\alpha$ - $\text{TiRuAs}$ /dry *tert*-butyl hydroperoxide system [34], in which the optimum catalyst amount that yielded maximum cyclohexene oxide selectivity and minimum cyclohex-2-en-1-ol and cyclohex-2-en-1-one selectivities was reported. When the applied catalyst content was beyond the critical amount, the aggregation among particles during

suspension might be more pronounced, resulting in loss of reactant accessibility into mesopores and subsequent lower catalytic activity. Additionally, it was mentioned that the complete absorption of water produced during the reaction can assist avoid the ring-opening of the epoxide from hydrolysis [35]. Therefore, the investigated amounts of catalyst are adequate to preserve the high catalytic performance without products from ring-opening. From these results, the optimum conditions for the reaction temperature and catalyst amount are 60 °C and 20 mg, respectively.

The concentration of H<sub>2</sub>O<sub>2</sub> was also another important parameter affecting the cyclohexene oxide selectivity to be further optimized. By fixing the substrate (cyclohexene) amount constant, the effect of H<sub>2</sub>O<sub>2</sub> amount was studied over a wide range of cyclohexene to H<sub>2</sub>O<sub>2</sub> molar ratio from 0.5 to 10 with the RuO<sub>2</sub>/TiO<sub>2</sub> catalyst (note that the previously described results were based on the ratio of 4). In order to compare the catalytic performance, the experiments without the RuO<sub>2</sub>/TiO<sub>2</sub> catalyst (control experiments) were also performed at various cyclohexene/H<sub>2</sub>O<sub>2</sub> ratios. In control experiments, the results from product determination reveal that the autooxidation of cyclohexene to form cyclohexene oxide and cyclohex-2-en-1-ol

but with relatively low conversion was observed. This is plausibly due to the strong oxidizing power of H<sub>2</sub>O<sub>2</sub>, where it reacts with *tert*-butanol to initially form the in situ generated *tert*-butyl hydroperoxide, which functions as a major source of the initiator and is then thermally decomposed to generate active free radicals for autooxidation reaction with cyclohexene in the presence of dissolved molecular O<sub>2</sub> acting as propagating species to finally produce those oxygen-containing products [28]. Fig. 6 represents the cyclohexene conversion and product selectivities at various cyclohexene/H<sub>2</sub>O<sub>2</sub> ratios both in the case of the absence and presence of the RuO<sub>2</sub>/TiO<sub>2</sub> catalyst. As obviously seen in the case of the presence of the catalyst, the cyclohexene conversion was almost independent of the cyclohexene/H<sub>2</sub>O<sub>2</sub> ratio in all cases at approximately 30–35% over the entire range. However, it is interestingly found that the cyclohexene oxide selectivity dramatically increased until leveling off beyond the ratio of 4 at maximum cyclohexene oxide selectivity of approximately 80% and vice versa for the cyclohex-2-en-1-ol selectivity, which noticeably declined until becoming almost unchanged at an identical value. In the meantime, the cyclohex-2-en-1-one selectivity was comparatively low only around 5–10% and its change was

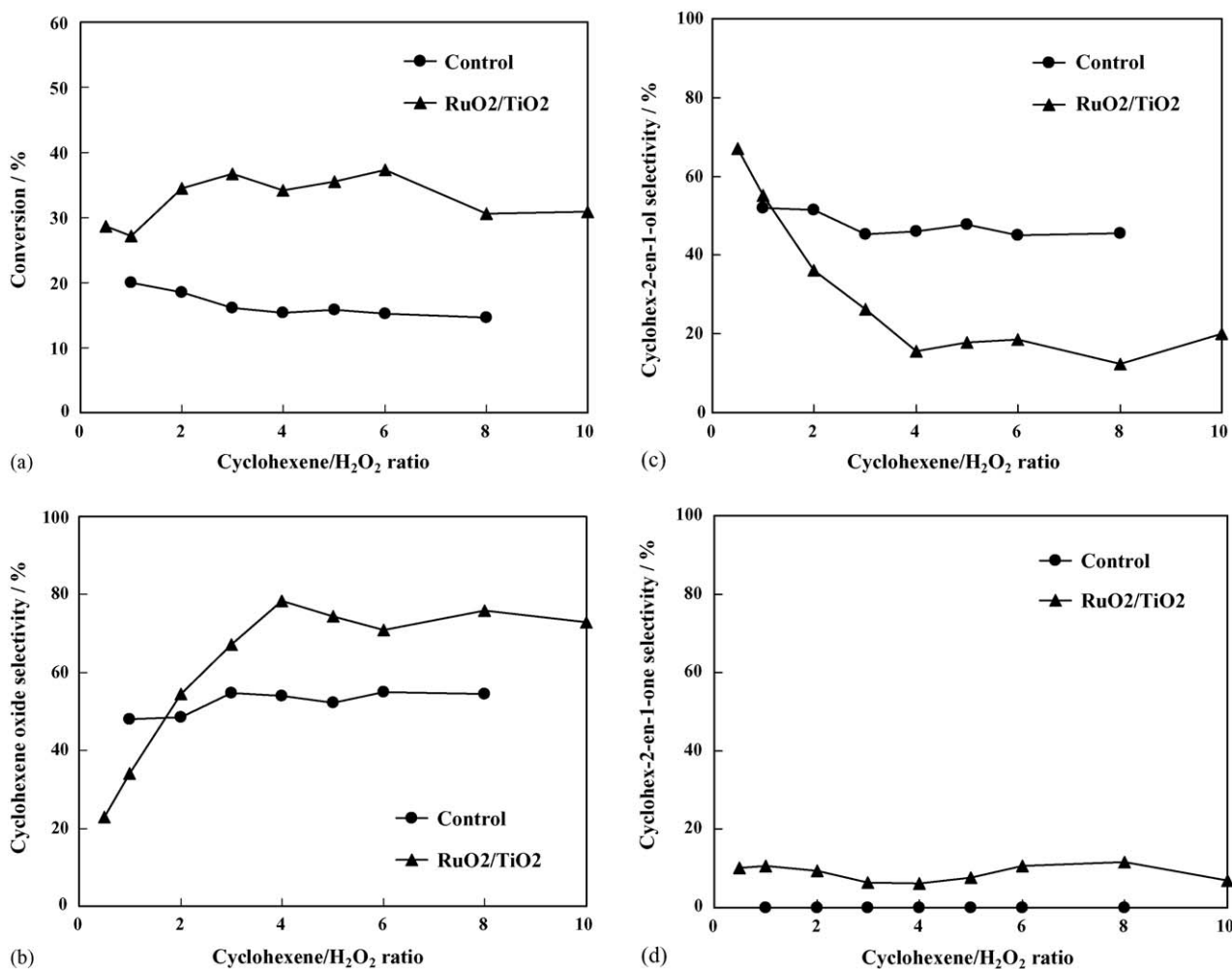


Fig. 6. Effect of cyclohexene/H<sub>2</sub>O<sub>2</sub> ratio on cyclohexene epoxidation catalyzed by RuO<sub>2</sub>/TiO<sub>2</sub> catalyst compared with control experiments: (a) cyclohexene conversion, (b) cyclohexene oxide selectivity, (c) cyclohex-2-en-1-ol selectivity and (d) cyclohex-2-en-1-one selectivity. Reaction conditions: cyclohexene, 5 mmol; *tert*-butanol, 5 ml; catalyst, 20 mg; reaction temperature, 60 °C; reaction time, 3 h.

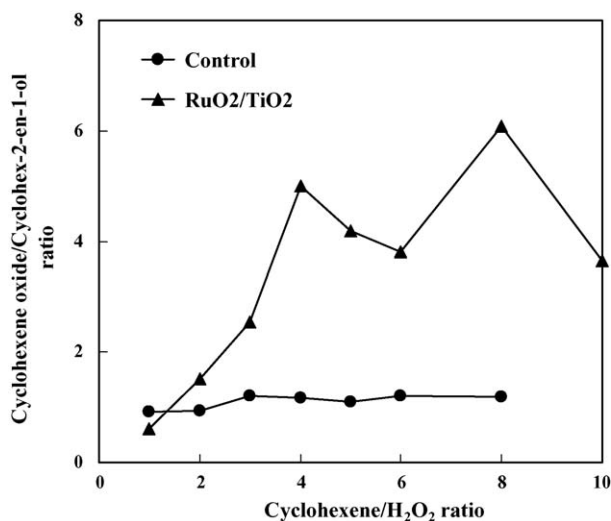


Fig. 7. Effect of cyclohexene/H<sub>2</sub>O<sub>2</sub> ratio on product (cyclohexene oxide/cyclohex-2-en-1-ol) ratio from cyclohexene epoxidation catalyzed by RuO<sub>2</sub>/TiO<sub>2</sub> catalyst compared with control experiments. Reaction conditions: cyclohexene, 5 mmol; *tert*-butanol, 5 ml; catalyst, 20 mg; reaction temperature, 60 °C; reaction time, 3 h.

much less than that of the other products. In contrast to the case of the presence of the catalyst, the cyclohexene conversion was relatively low around 15–20% in the case of the absence of the catalyst, whereas both the cyclohexene oxide and cyclohex-2-en-1-ol selectivities were almost at the similar level both at roughly 50% over the entire range of the cyclohexene/H<sub>2</sub>O<sub>2</sub> ratio. Besides, no cyclohex-2-en-1-one was observed at any conditions. Therefore, the cyclohexene/H<sub>2</sub>O<sub>2</sub> ratio of 4 is sufficient to attain satisfactorily high cyclohexene oxide selectivity.

Since the main products from the reaction are cyclohexene oxide (desired product) and cyclohex-2-en-1-ol (undesired product), it is worth demonstrating the product ratio to evaluate the catalytic performance of the catalyst in comparison with the case of control experiments at various cyclohexene/H<sub>2</sub>O<sub>2</sub> ratios. Fig. 7 shows the comparison of the cyclohexene oxide/cyclohex-2-en-1-ol ratio over the entire range of the cyclohexene/H<sub>2</sub>O<sub>2</sub> ratio. It is evident that especially beyond the cyclohexene/H<sub>2</sub>O<sub>2</sub> ratio of 4, the product ratio in the case of the RuO<sub>2</sub>/TiO<sub>2</sub> catalyst was much higher than that in the case of the control experiments without the catalyst, of which the product ratio was approximately 1 over the entire range of the cyclohexene/H<sub>2</sub>O<sub>2</sub> ratio. As can be seen from Figs. 6 and 7 in the case of the absence of the catalyst over such the entire range that both almost constant cyclohexene conversion and product (cyclohexene oxide and cyclohex-2-en-1-ol) selectivities with nearly the same molar product formation were observed, it can be supposed that the amount of dissolved molecular O<sub>2</sub>, which was likely to be consistent in all experiments, was the most decisive factor determining the autooxidation activity, although different contents of the in situ generated *tert*-butyl hydroperoxide were formed. However, in the case of the presence of the catalyst, it certainly plays a crucial role in overall catalytic performance due to the surface epoxidation upon oxygen transfer reaction. Since the particular amount of catalyst (20 mg, 0.25 mmol) was

used in the reaction conditions of excess *tert*-butanol, constant cyclohexene amount (5 mmol) and different H<sub>2</sub>O<sub>2</sub> amounts (decreasing from 10 to 0.5 mmol in order to obtain different cyclohexene/H<sub>2</sub>O<sub>2</sub> ratios increasingly ranging from 0.5 to 10), the active catalyst surface available for *tert*-butyl peroxotitanium complex formation prior to oxygen transfer reaction was then limited. At the cyclohexene/H<sub>2</sub>O<sub>2</sub> ratios lower than optimum value of 4, large amount of H<sub>2</sub>O<sub>2</sub> might be left in the solution phase, being able to react with cyclohexene via chain free radical reactions upon autooxidation pathway. In conjunction with the surface epoxidation reaction, this might eventually result in high cyclohex-2-en-1-ol selectivity and low cyclohexene oxide selectivity. On the contrary, at the cyclohexene/H<sub>2</sub>O<sub>2</sub> ratios more than optimum value of 4, the surface oxygen transfer reaction to form cyclohexene oxide as the main product might predominantly occur, while the difference due to autooxidation might be reasonably negligible because most of H<sub>2</sub>O<sub>2</sub> used probably underwent *tert*-butyl peroxotitanium complex formation for surface cyclohexene epoxidation. Consequently, the high cyclohexene oxide selectivity was attained with low undesired product selectivities, while the total amount of convertible cyclohexene through the combination of surface epoxidation and autooxidation at cyclohexene/H<sub>2</sub>O<sub>2</sub> ratios more than value of 4 might be insignificantly different, causing slight change in its conversion.

The recyclability test of the catalyst for cyclohexene epoxidation with H<sub>2</sub>O<sub>2</sub> in *tert*-butanol was also tested for three cycles at the obtained optimum reaction conditions. From the experimental results, it can be found that the cyclohexene conversion only slightly decreased, however the selectivity to cyclohexene oxide significantly decreased to 33 and 19% for the second and third cycles, respectively. Since the recyclability of the catalyst is very indispensable for real application, potential approaches to efficiently recover the spent catalyst should have to be essentially investigated in future work.

Finally, it can be concluded that at the optimum reaction conditions (reaction temperature, 60 °C; catalyst, 20 mg; cyclohexene/H<sub>2</sub>O<sub>2</sub> ratio, 4) under the investigated system, the RuO<sub>2</sub>-loaded nanocrystalline mesoporous TiO<sub>2</sub> was verified to be a promising catalyst with high catalytic performance for cyclohexene epoxidation with H<sub>2</sub>O<sub>2</sub>. However, the recyclability of the catalyst must be further evaluated.

#### 4. Conclusions

Nanocrystalline mesoporous TiO<sub>2</sub> catalyst with narrow monomodal pore size distribution was synthesized, loaded with 1 mol% RuO<sub>2</sub> by incipient wetness impregnation process, and utilized as an effective catalyst for cyclohexene epoxidation with H<sub>2</sub>O<sub>2</sub>. Several reaction parameters in the cyclohexene epoxidation reaction, namely reaction temperature, amount of catalyst and concentration of H<sub>2</sub>O<sub>2</sub> in terms of cyclohexene/H<sub>2</sub>O<sub>2</sub> ratio, were optimized to acquire maximum selectivity to cyclohexene oxide. Under optimization of these parameters, maximum cyclohexene oxide selectivity up to 80% was achieved when cyclohexene/H<sub>2</sub>O<sub>2</sub> ratio, catalyst amount and reaction temperature were 4, 20 mg and 60 °C, respectively.

## Acknowledgements

This work was financially supported by the Grant-in-aid for Scientific Research from the Ministry of Education, Science, Sports and Culture, Japan, under the 21COE program and the Nanotechnology Support Project. Grateful acknowledgments are forwarded to (1) Prof. S. Isoda and Prof. H. Kurata and (2) Prof. T. Yoko at Institute for Chemical Research, Kyoto University, for their continuous support of the use of TEM and XRD apparatus, respectively.

## References

- [1] A. Hagfeldt, M. Gratzel, *Chem. Rev.* 95 (1995) 49.
- [2] Z. Zhang, C.C. Wang, R. Zakaria, Y.J. Ying, *J. Phys. Chem. B* 102 (1998) 10871.
- [3] C.B. Almquist, P. Biswas, *J. Catal.* 212 (2002) 145.
- [4] L. Wu, J.C. Yu, X. Wang, L. Zhang, J. Yu, *J. Solid State Chem.* 178 (2005) 321.
- [5] F. Rouquerol, J. Rouquerol, K. Sing, *Adsorption by Powders and Porous Solids: Principles Methodology and Applications*, Academic Press, San Diego, 1999.
- [6] D.M. Antonelli, Y.J. Ying, *Angew. Chem. Int. Ed. Engl.* 34 (1995) 2014.
- [7] C.W. Jones, *Applications of Hydrogen Peroxide and Derivatives*, RSC, Cambridge, 1999.
- [8] R.A. Sheldon, M.C.A. van Vliet, in: R.A. Sheldon, H. van Bekkum (Eds.), *Fine Chemicals through Heterogeneous Catalysis*, Wiley, Weinheim, 2001.
- [9] W.R. Sanderson, *Pure Appl. Chem.* 72 (2000) 1289.
- [10] Technical Data Sheet, Chemical Divisions, BASF Corporation, 1997.
- [11] J.M. Fraile, J.I. García, J.A. Mayoral, E. Vispe, *Appl. Catal. A: Gen.* 245 (2003) 363.
- [12] K. Karakitsou, X.E. Verykios, *J. Catal.* 152 (1995) 360.
- [13] K. Gurunathan, P. Maruthamuthu, *Int. J. Hydrogen Energy* 20 (1995) 287.
- [14] G.R. Bamwenda, H. Arakawa, *Appl. Catal. A: Gen.* 210 (2001) 181.
- [15] J. Sato, N. Saito, H. Nishiyama, Y. Inoue, *J. Photochem. Photobiol. A: Chem.* 148 (2002) 85.
- [16] P.K. Dutta, A.S. Vaidyalingam, *Micropor. Mesopor. Mater.* 62 (2003) 107.
- [17] J. Qin, K. Aika, *Appl. Catal. B: Environ.* 16 (1998) 261.
- [18] S. Hosokawa, H. Kanai, K. Utani, Y. Taniguchi, Y. Saito, S. Imamura, *Appl. Catal. B: Environ.* 45 (2003) 181.
- [19] B. Scharbert, E. Zeisberger, E. Paulus, *J. Organomet. Chem.* 493 (1995) 143.
- [20] R.I. Kureshy, N.H. Khan, S.H.R. Abdi, P. Iyer, *J. Mol. Catal. A: Chem.* 124 (1997) 91.
- [21] R. Antony, G.L. Tembe, M. Ravindranathan, R.N. Ram, *Polymer* 39 (1998) 4327.
- [22] B. Cetinkaya, E. Cetinkaya, M. Brookhart, P.S. White, *J. Mol. Catal. A: Chem.* 142 (1999) 101.
- [23] D.C. Sherrington, *Catal. Today* 57 (2000) 87.
- [24] K. Jitsukawa, Y. Oka, H. Einaga, H. Masuda, *Tetrahedron Lett.* 42 (2001) 3467.
- [25] V.R. de Souza, G.S. Nunes, R.C. Rocha, H.E. Toma, *Inorg. Chim. Acta* 348 (2003) 50.
- [26] D. Chatterjee, S. Basak, A. Mitra, A. Sengupta, J. Le Bras, J. Muzart, *Catal. Commun.* 6 (2005) 459.
- [27] T. Sreethawong, Y. Suzuki, S. Yoshikawa, *J. Solid State Chem.* 178 (2005) 329.
- [28] T. Sreethawong, Y. Yamada, T. Kobayashi, S. Yoshikawa, *J. Mol. Catal. A: Chem.* 241 (2005) 23.
- [29] J.C. Yu, J. Yu, W. Ho, L. Zhang, *Chem. Commun.* 19 (2001) 1942.
- [30] J. Yu, J.C. Yu, M.K.P. Lueng, W. Ho, B. Cheng, X. Zhao, J. Zhao, *J. Catal.* 217 (2003) 69.
- [31] Y. Zhang, A. Weidenkaff, A. Reller, *Mater. Lett.* 54 (2002) 375.
- [32] Y. Zhang, H. Zhang, Y. Xu, Y. Wang, *J. Solid State Chem.* 177 (2004) 3490.
- [33] Y.V. Kolen'ko, V.D. Maximov, A.V. Garshev, P.E. Meskin, N.N. Oleynikov, B.R. Churagulov, *Chem. Phys. Lett.* 388 (2004) 411.
- [34] S. Khare, S. Shrivastava, *J. Mol. Catal. A: Chem.* 217 (2004) 51.
- [35] D. Mandelli, M.C.A. van Vliet, R.A. Sheldon, U. Schuchardt, *Appl. Catal. A: Gen.* 219 (2001) 209.